Journal of Bioenergetics and Biomembranes, Vol. 31, No. 6, 1999

Structural Basis of Multifunctional Bovine Mitochondrial Cytochrome bc_1 Complex

Chang-An Yu,[1,3] Hua Tian,[1] Li Zhang,[1] Kai-Ping Deng,[1] Sudha K. Shenoy,[1] Linda Yu,[1] Di Xia,[2,4] Hoeon Kim,[2] and Johann Deisenhofer[2]

Received April 2, 1999

The mitochondrial cytochrome bc_1 complex is a multifunctional membrane protein complex. It catalyzes electron transfer, proton translocation, peptide processing, and superoxide generation. Crystal structure data at 2.9 A resolution not only establishes the location of the redox centers and inhibitor binding sites, but also suggests a movement of the head domain of the iron–sulfur protein (ISP) during bc_1 catalysis and inhibition of peptide-processing activity during complex maturation. The functional importance of the movement of extramembrane (head) domain of ISP in the bc_1 complex is confirmed by analysis of the *Rhodobacter sphaeroides* bc_1 complex mutants with increased rigidity in the ISP neck and by the determination of rate constants for acid/base-induced intramolecular electron transfer between [2Fe–2S] and heme c_1 in native and inhibitor-loaded beef complexes. The peptide-processing activity is activated in bovine heart mitochondrial bc_1 complex by nonionic detergent at concentrations that inactivate electron transfer activity. This peptide-processing activity is shown to be associated with subunits I and II by cloning, overexpression and *in vitro* reconstitution. The superoxide-generation site of the cytochrome bc_1 complex is located at reduced b_L and $Q^{\bullet -}$. The reaction is membrane potential-, and cytochrome *c*-dependent.

KEY WORDS: Cytochrome bc_1 complex; electron transfer reaction: mitochondrial-processing peptidase; superoxide-generation activity; electron transfer inhibitors.

INTRODUCTION

Bovine heart mitochondrial cytochrome bc_1 complex (ubiquinol:cytochrome *c* reductase or Complex III), which catalyzes electron transfer from ubiquinol to cytochrome *c*, has been crystallized in different forms (Yu *et al.*, 1996). The molecular structures of these crystals have been determined at around 3 A resolution (Xia *et al.*, 1997; Zhang *et al.*, 1998; Iwata *et al.*, 1998). This complex contains four redox prosthetic groups: cytochromes b_{566} (b_L) and b_{562} (b_H) cytochrome c_1, and a high-potential iron–sulfur cluster [(2Fe–2S)]. It contains eleven proteins with known amino acid sequences. The three (subunits III, IV, and V), which house *b*-type cytochromes, cytochrome c_1, and the iron–sulfur cluster, respectively, are essential subunits, while the eight (subunits I, II, VI–XI) containing no redox prosthetic groups are termed supernumerary subunits. The complex consists of 2165 amino acid residues with a total molecular mass of 248 kDa, not including approximately forty molecules of bound phospholipid (Yue *et al.*, 1991).

The three-dimensional (3-D) structure of mitochondrial bc_1 complex not only established the location of the redox centers and inhibitor binding sites but also suggested some unexpected features of the complex,

[1] Department of Biochemistry and Molecular Biology, Oklahoma State University, Stillwater, Oklahoma 74078-3035.
[2] The Howard Hughes Medical Institute and Department of Biochemistry, University of Texas Southwestern Medical Center, Dallas, Texas 75235.
[3] Author to whom correspondence should be addressed. Email: cayuq@okway.okstate.edu.
[4] Present address: Laboratory of Cell Biology, National Cancer Institute, National Institutes of Health, Bethesda, Maryland 20892.

0145-479X/99/0600-0191$16.00/0 © 1999 Plenum Publishing Corporation

which are: movement of the head domain of the iron–sulfur protein (ISP) during bc_1 catalysis (Xia *et al.*, 1997; Iwata *et al.*, 1998; Zhang *et. al.*, 1998; Kim *et al.*, 1998); close interaction between two symmetric related monomers (Xia *et al.*, 1997); and inhibition of the mitochondrial-processing peptidase (MPP) activity by the binding of subunit IX at the active site of MPP, located in interface of the subunits I and II.

In this review, we briefly summarize the structures of three different crystalline forms of the mitochondrial bc_1 complex, present biochemical evidence for the functional importance of ISP extramembrane domain movement in the electron transfer reaction, and discuss structure–function relationships of other activities associated with this complex.

STRUCTURE OVERVIEW

Bovine heart mitochondrial cytochrome bc_1 complex has been crystallized in different forms under different crystallization conditions (Yu *et al.*, 1996). Crystals grown in the presence of 20% glycerol diffracted X-rays to 2.6 A resolution using a synchrotron X-ray source. The first reported mitochondrial bc_1 crystal structure was solved at 2.9 A resolution using the MIRAS method with seven heavy atom derivatives (Xia *et al.*, 1997). The crystals have the symmetry of space group $I4_122$ with unit cell dimensions of $a = b = 153.5$ A and $c = 597.7$ A, with one bc_1 monomer in the crystallographic asymmetric unit. Each monomer consists of eleven different protein subunits. The complex exists as a dimer in the crystal. Closely interacting monomers are arranged as symmetric dimers and form cavities through which substrate or inhibitor binding pockets can be accessed. Structures of crystals with different space groups, $P2_12_12_1$ of chicken heart (Zhang *et al.*, 1998) and $P6_5$ and $P6_522$ of beef heart (Iwata *et al.*, 1998) were subsequently reported.

As shown in Fig. 1, the cytochrome bc_1 complex can be divided into three regions: matrix, transmembrane helix, and intermembrane space. There is no significant difference between the three reported structures. In fact, they are complementary, with tetragonal crystals ($I4_122$) having better resolution in the matrix and transmembrane regions, and hexagonal and orthorhombic crystals ($P6_5$ and $P6_522$ of beef heart and $P2_12_12_1$ of chicken heart) having better density in the intermembrane space region.

More than one-half of the molecular mass is located in the matrix region of the molecule, extending 75 A from the transmembrane helix. This region consists of subunits I, II, VI, part of subunit VII, the C-terminal portion of cytochrome c_1, the N-terminal portion of ISP, and subunit IX. Subunits I and II are structurally similar, each consisting of two domains of roughly equal size and identical folding topology.

The transmembrane helix region is about 42 A thick. It consists of 13 transmembrane helixes in each monomer, eight from cytochrome *b*, with the remaining five belonging to cytochrome c_1, ISP, and subunits VlI, X, and XI. Atomic models of all the subunits have been built. The transmembrane region of cytochrome *b* houses heme b_L, heme b_H, and the Q_o and Q_i pockets.

The intermembrane space region, which extends 38 A into the cytoplasm from the membrane surface, houses the functional domains of cytochrome c_1 and ISP, as well as subunit VIII. The extramembrane domain of ISP in one monomer is connected to the tail domain of this protein in the other monomer. This intertwining structure of two ISPs in the symmetrically related monomers suggests that the functional enzyme complex exists as a dimer. The structure of the extramembrane domain of ISP is virtually identical to that of the reported truncated protein (Iwata *et al.*, 1996) in the reduced state.

The N-terminal part of cytochrome c_1 is an all α-helix-type protein; its structure resembles Type I cytochrome *c*. Heme c_1 is ligated with Cys37 and Cys40. The carboxy group of one of the propionates of heme c_1 forms a salt bridge with Arg120. The other propionate forms a hydrogen bond with His161 of ISP in $P6_522$ (Iwata *et al.*, 1998), whereas it is free in other crystal forms. In the $P6_522$ crystal, the [2Fe–2S] is closest to heme c_1, suggesting that electron transfer between the [2Fe–2S] and heme c_1 may take place in this conformation.

The positions of the four redox iron centers within the bc_1 complex and the binding sites of specific respiratory inhibitors have been identified. In all crystal forms, the distance between the hemes of cytochromes b_L and b_H is 21 A, in good agreement with the prediction of 22 A, based on the putative heme ligands in the primary sequence (Widger *et al.*, 1984), and with the spin relaxation of the b_H and b_L in EPR studies (Ohnishi *et al.*, 1989). The distance between the heme b_L of the two monomers is less than 21 A, indicating close interaction between these two hemes and providing further support for the existence of a functional dimer in the cytochrome bc_1 complex. However, the distances between [2Fe–2S] and the hemes of cytochromes c_1 and b_L in different crystal forms are vari-

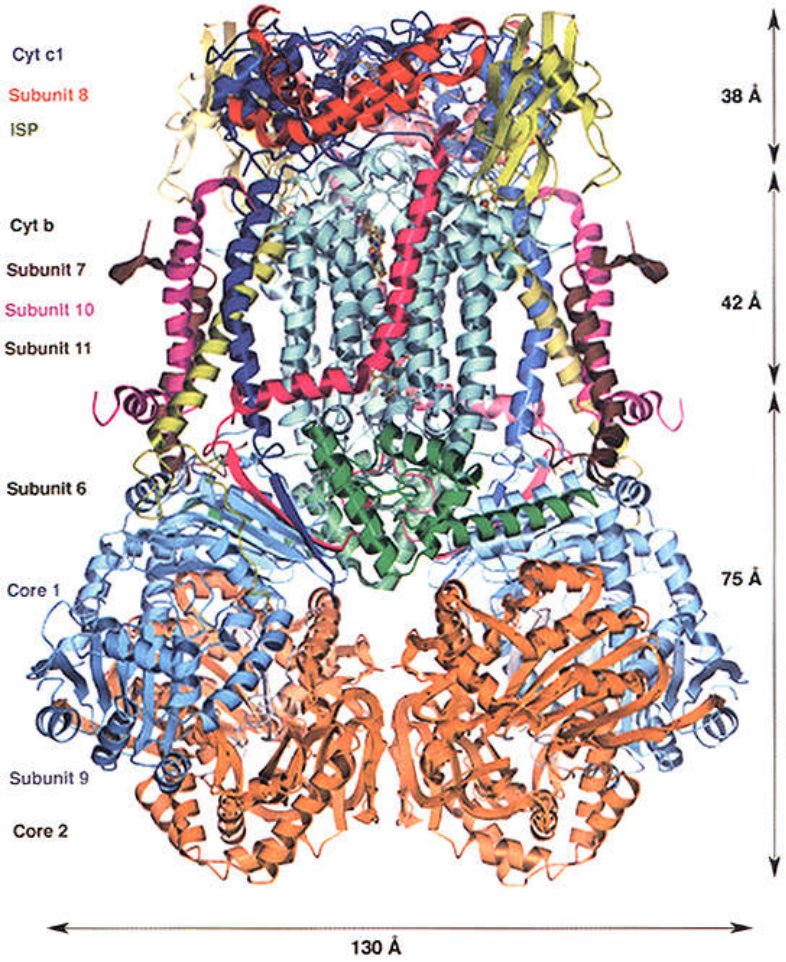

Fig. 1. Structural model of the dimeric bovine mitochondrial cytochrome bc_1 complex. The polypeptides are drawn as ribbons and heme moieties as ball-and-stick models. The top of the diagram is in the mitochondrial intermembrane space; the bottom is in the mitochondrial matrix space.

able. They are 31 and 27 A, respectively, in tetragonal $I4_122$ crystals (Xia *et al.*, 1997) and 15.5 and 35.5 A, respectively, in hexagonal $P6_522$ crystals (Iwata *et al.*, 1998). The bc_1 complex in tetragonal $I4_122$ crystals is fully oxidized while the redox state of hexagonal crystals has not been rigorously established. Moreover, the crystal contacts in tetragonal crystals ($I4_122$) are at subunit II, while in hexagonal crystals ($P6_5$ and $P6_522$) they are at the extramembrane domain of ISP. It is unclear, at present, whether the shorter distance between the [2Fe−2S] and heme c_1 in hexagonal crystals results from crystal contacts or from the partial reduction of heme c_1 or [2Fe−2s] in the crystals.

The position of [2Fe−2S] changes during the binding of different Q_o site inhibitors. In tetragonal $I4_122$ crystals, binding of stigmatellin or 5-undecyl-6-hydroxy-4,7-dioxobenzothiazole (UHDBT) enhances the electron density of the anomalous scattering peak of [2Fe−2S], suggesting that these inhibitors arrest the mobility of ISP (Kim *et al.*, 1998) at a fixed position, which is 27 A from heme b_L and 31 A from heme c_1. Conversely, binding of E-b-methoxyacrylate-stilbene (MOAS) or myxothiazol to the complex abolishes the electron density of the anomalous scattering peak of [2Fe−2S], suggesting that these inhibitors increase the mobility of ISP to a released state in the crystal (Kim *et al.*, 1998) somewhere between heme c_1 and heme b_L (no definitive position). In orthorhombic $P2_12_12_1$ crystals of chicken enzyme, binding of stigmatellin shifts [2Fe−2S] from the "c_1-position" to the "*b*-position"(Zhang *et al.*, 1998). The *b*-position in the $P2_12_12_1$ crystal happened to be the same as the " fixed"position

observed in tetragonal $I4_122$ crystals (Xia *et al.*, 1997). In bovine $P6_5$ crystals, the [2Fe–2S] is located between the positions of the *b*- and the c_1-state. The observation of more than two positions of [2Fe–2S] in $P6_5$ crystals supports the idea of one fixed position and other released (loose) positions, suggested for the $I4_122$ structure (Kim *et al.*, 1998).

ELECTRON TRANSFER AND PROTON TRANSLOCATION

Movement of Extramembrane Domain of ISP

Structural Evidence

The movement of the head domain of ISP during bc_1 catalysis was first indicated by the observation of low electron density in the region of the extramembrane domain of ISP (Xia *et al.*, 1997) in tetragonal $I4_122$ crystals. Further support came from the observation of varying positions for [2Fe–2S] in different crystal forms and in complexes loaded with different inhibitors (Zhang *et al.*, 1998; Iwata *et al.*, 1998; Kim *et al.*, 1998). Since the extramembrane domain of ISP in the reduced form is known to be rigid (Link and Iwata, 1996), these variable positions of [2Fe–2S] must result from movement of the whole domain. It should be noted that the rigidity of the oxidized form of ISP has not yet been established.

Functional Evidence

The X-ray crystallographic studies clearly show that the position of [2Fe–2S] varies in different crystal forms and is affected by binding of different Q_o site inhibitors. However, these studies do not give direct proof of the functional significance of such movement. For this, we turn to data generated by molecular genetic manipulation of the bacterial cytochrome bc_1 complex. Since both the extramembrane and transmembrane domains of ISP are rigid, movement of the extramembrane domain requires flexibility in the neck region of the protein. As indicated in Table I, decreasing the flexibility of the neck region by introducing proline substitutions or other amino acid deletions, greatly reduced electron transfer activity and increased the activation energy of the reaction (Tian *et al.*, 1998). Formation of a disulfide bond between two engineered cysteines (see Fig. 2), separated by only one amino acid residue, in the neck region near the transmembrane helix, drastically reduced electron transfer activity (Tian *et al.*, 1999). Release of the disulfide bond, by reduction or alkylation of the regenerated cysteines, restores activity to a level comparable to that of the wild-type enzyme (Tian *et al.*, 1999).

Table I. Characterization of ISP Neck[f] Mutants *Rhodobacter sphaeroides*

Mutations	Photo-synthetic growth	Enzymatic activity[a] Chroma-tophore	ICM[b]	Purified complex
Complement	++[c]	2.2	2.1	2.5
ΔADV	+	0.2	0.2	0
ALA–PLP	++	0.7	—	0.7
ADV–PPP	—	—	0	0
PSA–CSC	—[d]	—	0	0
ADV–CDC	+	1.5	0	0
PSA–CSC + β-ME			1.2	—
(PSA–CSC + β-ME) + NEM[e]		—	1.2	—
ADV–CDC + β-ME		1.5	1.4	—
(ADV–CDC + β-ME) + NEM		1.5	1.4	—

[a] Enzymatic activity is expressed as μmol cytochrome *c* reduced/min/nmol cytochrome *b*.
[b] Intracytoplasmic membrane (ICM) was prepared from cell undergoing semiaerobic or aerobic growth conditions, in which the cyclic electron transfer pathway is not obligatory. Mutated *bc*1 complex with no enzymatic activity can still be overexpressed and characterized in the ICM membrane.
[c] The growth phenotype is essentially the same as the wild type.
[d] No photosynthetic growth within 4 days.
[e] Five fold excess amount of *N*-ethylmaleimide was added to the β-ME treated membrane.
[f] Neck residues 39–48, -NPSADVQALA-.

pH Induced Intramolecular Electron Transfer of the Native and Inhibitor-Loaded Complexes

The fact that the midpoint potential of ISP is pH dependent, while that of cytochrome c_1 is not, allows us to measure intramolecular electron transfer between [2Fe–2S] and heme c_1 in the native and inhibitor-treated bc_1 complexes by adjusting the pH of the enzyme solution. At pH 8, ISP and cytochrome c_1 have about the same degree of reduction, as they have the same midpoint potential. The midpoint potential of [2Fe–2S] increases as pH decreases. When a cytochrome c_1–partially reduced bc_1 complex, at pH 8.0, is mixed with a buffer of higher pH, cytochrome c_1 becomes more reduced, at the expense of the oxidation of ISP, and

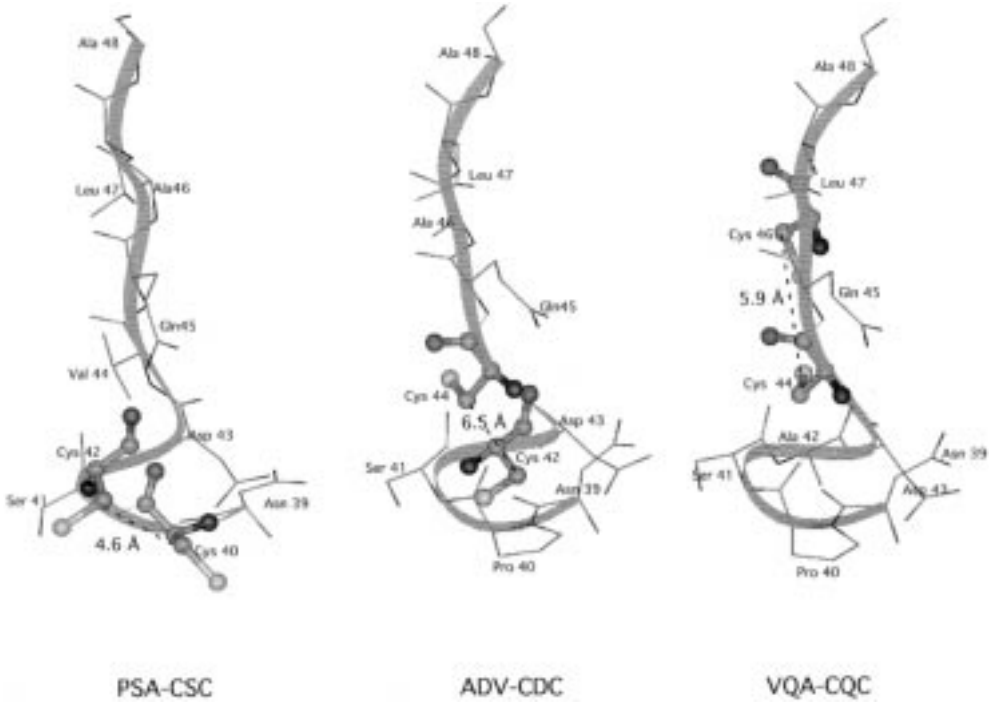

Fig. 2. The distance between two cβ atoms of the introduced cysteine residues of the double cysteine mutants. The distance for the disulfide bond between Cys160 and Cys140 in bovine ISP head domain is 4–4.5 A. The distance listed above are deduced from molecular modeling of these double cysteine substitutions. Mutant PSA-CSC is the easiest one to form disulfide bond.

reaches maximal reduction at pH 9.4. On the other hand, when the complex is mixed with a buffer of lower pH, oxidation of cytochrome c_1 is observed. The rates of these pH-induced electron transfers are greater than what can be determined accurately by a conventional stopped-flow apparatus, suggesting that either [2Fe–2S] lies close to or can easily move to heme c_1 when only one of the two redox centers is in the reduced state. When similar experiments are carried out with the UHDBT-treated complex, the rate of electron transfer is reduced to a $t_{1/2}$ of 2 sec, when increasing the pH from 7.5 to 9.0. An even lower rate is observed for the stigmetallin-treated complex. These results suggest that UHBDT and stigmatellin are capable of arresting [2Fe–2S] at a "fixed" position, 31 A away from heme c_1. However, MOAS has little effect on the rate of pH-induced electron transfer between these two centers. This is consistent with structural data that indicates binding of MOAS at cytochrome *b* enhances the mobility of the extramembrane domain of ISP to a "released" position, somewhat closer to heme c_1, facilitating electron transfer. Since the released-state position of [2Fe–2S] is observed in the fully oxidized crystals, [2Fe–2S] may occupy a different position in the partially reduced complex. It will not be surprising to find that partially reduced [2Fe–2S] is at a position as close to heme c_1 as it is in the "*c*-state" of hexagonal crystals. As expected, antimycin has no effect on the rate of intramolecular electron transfer between c_1 and [2Fe–2S] since its binding does not affect the position of [2Fe–2S].

Electron Transfer at the Q_o Site

Key features of the Q-cycle mechanism for electron transfer and proton translocation are the bifurcation of quinol oxidation at the Q_o site (Mitchell, 1976; Trumpower, 1990) and quinone reduction at a separate Q_i site. Experimental evidence suggests that the [2Fe–2S] of ISP is reduced by ubiquinol at the Q_o site. However, it is unclear as to why the more oxidizable ubisemiquinone formed does not further reduce [2Fe–2S]. Instead, it reduces the thermodynamically less favorable heme b_L. With a mobile ISP extramembrane domain, it is possible that the [2Fe–2S], reduced by the first electron of quinol, either can not donate an electron to cytochrome c_1 (because of 31 A distance) before the second electron of ubiquinol is transferred

to heme b_L (Yu *et al.*, 1998), or the reoxidized ISP (assuming reduced FeS can move close to heme c_1) is unable to return to its original position, to be rereduced (Brandt, 1998), before the electron of semiquinone is transferred to heme b_L. It is tempting to speculate that the change of the quinol-binding site to a semiquinone-binding site (Yu *et al.*, 1998; Brandt, 1998), and reduction of heme b_L, causes a conformational change in cytochrome *b* which allows ISP to move close enough to heme c_1 to facilitate rapid electron transfer. This would also explain why ubisemiquinone, a powerful reductant, reduces heme b_L, but not [2Fe–2S], during quinol oxidation. The absence of detectable ubisemiquinone during catalysis (Junemann *et al.*, 1998), however, undermines this hypothesis.

An alternative hypothesis for the electron transfer event at the Q_o site is that the electron donor for [2Fe–2S] is a ubiquinol heme b_L complex, rather than ubiquinol itself (Yu *et al.*, 1998). Once the first electron of ubiquinol in the complex is transferred to [2Fe–2S], the second electron immediately transfers to heme b_L and then to heme b_H. In this scenario, no ubisemiquinone is generated. The close proximity of the heme b_L of one monomer to the heme b_L of the other monomer may facilitate the transfer of the second electron to heme b_L. Electron transfer from heme b_L to heme b_H results in a conformational change in cytochrome *b*, which makes (or allows) the reduced ISP to move closer to heme c_1, allowing electron transfer to take place. In this way, the second electron of ubiquinol may reach its destination, b_H or Q at the Q_i site, before or at the same time as the first electron reaches heme c_1. Since the exact nature of ubiquinol binding in the Q_o pocket is unknown, the deprotonation (Ugulava and Crofts, 1998; Brandt and Okun, 1997; Denke *et al.*, 1998) of ubiquinol in the reaction sequence remains to be elucidated.

Electron Transfer at the Q_i Site

Binding of ubiquinone at the Q_i site is indicated by the observation of a quinone-shaped negative electron density near heme b_H in the antimycin loaded bc_1 complex crystal (Xia *et al*, 1997). This negative density overlaps with that of antimycin. A positive quinone density was recently identified in a native bc_1 complex crystal. Here, ubiquinone is closely bound to heme b_H, within 5 A of the edge of the heme tetrapyrrol. Therefore, electron transfer between Q and heme b_H and vice versa, should take place at a high rate. One of the carbonyl groups of quinone is very close to an aspartate residue (D228), which may play a role in protonation, after quinone is reduced.

Proton Translocation

Although the Q-cycle hypothesis explains well the $2H^+/e$ stoichiometry of proton transfer, and the structural information obtained so far generally supports this hypothesis, the proton transfer path in the bc_1 complex, during ubiquinol oxidation, is still not clear. No obvious proton channel has been found in the cytochrome bc_1 complex at the current level of structural resolution. Since the simplest bacterial bc_1 complex has no supernumeral subunits and has full proton translocation function, proton translocation must be achieved through transmembrane helixes of cytochrome *b*, cytochrome c_1, and ISP. The van der Waals surface of the matrix side of these transmembrane helixes, particularly in cytochrome b, shows several openings for proton uptake from the matrix. The van der Waals surface of the intermembrane surface is totally sealed: proton exit through this region requires some sort of conformational change or gating device. Available biochemical data indicate that the ligands of the [2Fe–2S] of ISP may play an essential role in proton exit. It has been reported (Miki *et al.*, 1990) that the [2Fe–2S] of ISP is lost when one of the histidine ligands is destroyed during illumination of the hematoporphyrin-treated complex. The resulting complex leaks protons when reconstituted into phospholipid vesicles. The redox state-dependent pK_a of the [2Fe–2S] histidine ligands also suggests that these ligands may be involved in proton release (Link and Iwata, 1996). Cytochrome bc_1 complexes depleted in ISP, prepared by biochemical methods or by genetic manipulation, form proton-leaking vesicles when embedded in phospholipid vesicles, lending further support for an ISP ligand-dependent proton translocation.

MITOCHONDRIAL PROCESSING PEPTIDASE (MPP) ACTIVITY IN BOVINE HEART MITOCHONDRIAL CYTOCHROME bc_1 COMPLEX

In addition to the sequence homology between subunits I and II of bovine bc_1 complex and α and β

subunits of MPP, a sequence of Y91XXE94 $H95(X)_{76}E171$ (Xia *et al.*, 1997), similar to the zinc-binding motif $HXXEHX_{76}E$, in the β-subunit of MPP, is present in subunit I of the bovine enzyme. Furthermore, residues K_{300} and R_{301} of the bovine subunit II are structurally close to the putative zinc-binding motif in subunit I and may contribute to the active site (see Fig. 3). However, no MPP activity is detected in the active bovine cytochrome bc_1 complex. Based on 3-D structural information, the lack of MPP activity in the bovine complex appears to be due to the binding of subunit IX at the active site of MPP in subunits I and II. This is, indeed, the case because when crystalline bc_1 complex is treated with nonionic detergents such as Triton X-100, electron transfer activity is lost while MPP activity appears. Triton X-100 disrupts the structural integrity of the complex and weakens the binding of the inhibitory polypeptide to subunits I and II, thus activating MPP activity (Deng *et al.*, 1998). When synthetic polypeptides composed of various lengths of the C-terminal end of presequences and the N-terminal end of mature protein of nuclear encoded subunits are used as substrate, the specificity of MPP is found to be governed more by the length of the N-terminal end of the mature subunit than by the length of the C-terminal end of the presequence. This is not in line with a consensus presequence motif of RXΦXXS being the MPP cleavage site (Von Heijne *et al.*, 1989). Although MPP activity is not stimulated by the addition of divalent cations, it is inhibited by the addition of EDTA. The EDTA-inhibited activity is restored by the addition of divalent cations, indicating that divalent cations are essential.

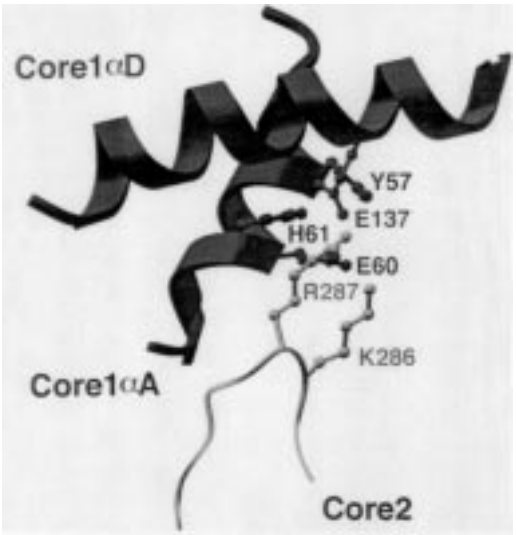

Fig. 3. The 3-D structure of the bc_1 complex in subunits I and II containing the putative MPP active site. The amino acid residue numbers are based on the sequence of mature protein.

To further confirm that the MPP activity is associated with subunits I and II of the bovine complex, we have obtained purified recombinant proteins and tested them for MPP activity individually or in combination. The cDNAs encoding subunits I and II of the bovine bc_1 complex were amplified from a bovine heart cDNA library using PCR, cloned into the expression vector, $pET30^{a+}$, and overexpressed as *His*-tagged fusion proteins in *E. coli* (Shenoy *et al.*, 1998). Recombinant subunits I and II were purified to homogeneity from soluble cell-free extracts using a Ni–NTA resin. Purified recombinant subunit I or II alone has no MPP activity. However, when these two recombinant proteins are mixed together, MPP activity appears (Shenoy *et al.*, 1998). Maximum activity is obtained when the molar ratio of these two proteins reaches one. Like the MPP activity in Triton X-100-treated bc_1 complex, the reconstituted MPP activity is stimulated by the addition of divalent cations and inhibited by EDTA. These results clearly indicate that Triton-X100 activated MPP activity is associated with subunits I and II of the complex.

SUPEROXIDE-GENERATING ACTIVITY OF THE CYTOCHROME bc_1 COMPLEX

It has been reported that about 1-2% of oxygen consumption during respiration is not involved with oxidative phosphorylation, but rather with the formation of superoxide (Boveris *et al.*, 1972). Generation of superoxide during respiration has two physiological purposes: regulation of membrane potential and maintenance of body temperature. Production of superoxide anion ($O_2^{\cdot -}$), measured as the chemiluminescence of MCLA [2-methyl-6-(*p*-methoxyphenyl)-3,7-dihydroimidazo[1,2-a]pyrazin-3-one hydrochloride]-$O_2^{\cdot -}$, is observed during electron transfer from succinate to cytochrome *c* by reconstituted succinate: cytochrome *c* reductase-phospholipid vesicles replenished with succinate dehydrogenase (Zhang *et. al.*, 1998). Cytochrome bc_1 vesicles are not suitable for studies of $O_2^{\cdot -}$ generation because ubiquinol alone is capable of producing $O_2^{\cdot -}$ in the presence of cytochrome *c*. Addition of FCCP or detergent to the reconstituted reductase-PL vesicles abolishes $O_2^{\cdot -}$ production, suggesting that $O_2^{\cdot -}$ production is a result of the membrane potential generated during electron transfer through

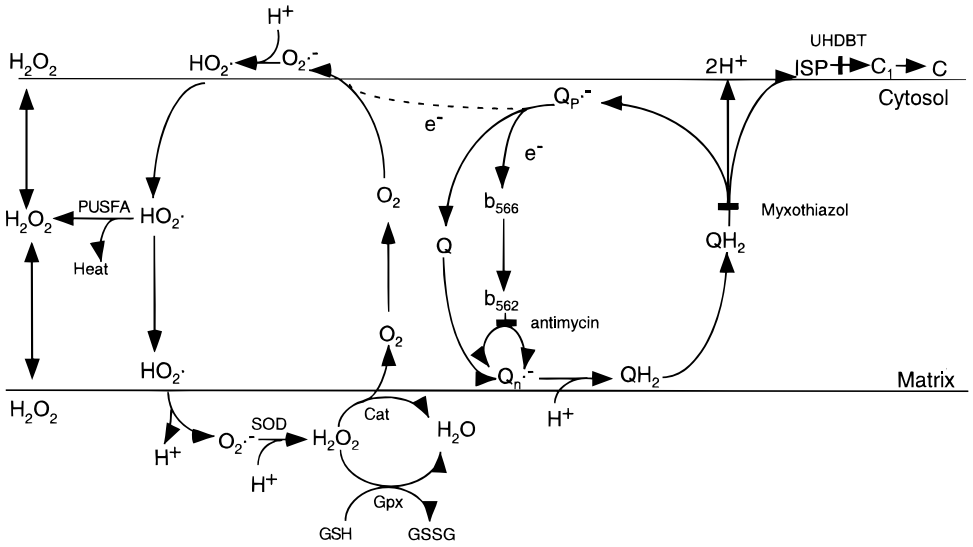

Fig. 4. Relationship between proton motive Q-cycle and the membrane potential regulating superoxide cycle in the cytochrome bc_1 region of the respiratory chain. Abbreviations used are: SOD, superoxide dismutase; PUSFA, polyunsaturated fatty acyl groups of lipids; UHDBT, 5-undecyl-6-hydroxyl-4,7-dioxobenzothiazol; Gpx, glutathione peroxidase; Cat, catalase. GSH and GSSG are reduced and oxidized glutathione respectively.

the cytochrome bc_1 complex. Production of $O_2^{\cdot -}$ is also observed during electron transfer from succinate to cytochrome *c* by antimycin-treated reductase in which 99.7% of the reductase activity is inhibited. The rate of $O_2^{\cdot -}$ production is closely related to the rate of antimycin-insensitive cytochrome *c* reduction. Factors affecting antimycin-insensitive reduction of cytochrome *c* also affect $O_2^{\cdot -}$ production and vice versa. When the oxygen concentration in the system is decreased, the rate of superoxide anion production and cytochrome *c* reduction by antimycin-treated reductase decreases. When the concentrations of MCLA and cytochrome *c* are increased, the rate of $O_2^{\cdot -}$ production and cytochrome *c* reduction by antimycin-treated reductase increase. The rate of antimycin-insensitive cytochrome *c* reduction is sensitive to Q_o site inhibitors such as UHDBT. These results indicate that generation of $O_2^{\cdot -}$ during the oxidation of ubiquinol by the cytochrome bc_1 complex results from a leakage of the second electron of ubiquinol from its Q-cycle electron transfer pathway and its interaction with oxygen. Figure 4 shows the relationship between the Q cycle and the superoxide cycle hypotheses (Huang, 1993). The electron-leakage site is located at the reduced cytochrome b_{566} or ubisemiquinone of the Q_o site, as addition of MCLA to antimycin-treated cytochrome bc_1 complex, in the presence of catalytic amounts of succinate-cytochrome *c* reductase, delays cytochrome *b* reduction by succinate.

ACKNOWLEDGMENTS

The work described in this review was supported in part by Grant GM3072 from the National Institutes of Health; by Grant-in-Aid 9507873S from the American Heart Association and by Agricultural Experimental Station Project 1819, Oklahoma State University. J. D. is an investigator of Howard Hughes Medical Institute. We are grateful to Dr. Roger Koeppe for critical reading of this review.

REFERENCES

Boveris, A., Oshino, N., and Chance, B. (1972). *Biochem. J.* **128**, 617–630.
Brandt, U. (1998). *Biochim. Biophys. Acta* **1275**, 41–46.
Brandt, U. and Okun, J. U. (1997). *Biochemistry* **36**, 11234–11240.
Denke, E., Merbitz-Zahradnik, T., Hatzfeld, O., Snyder, C. H., Link, T. A., and Trumpower, B. L. (1998). *J. Biol. Chem* **273**, 9085–9093.
Deng, K.-P, Zhang, L., Kachurin, A. M., Yu, L., Xia, D., Deisenhofer, J., and Yu, C. A. (1998). *J. Biol. Chem.* **273**, 20752–20757.
Huang, T. (1993). Ph.D. Thesis, Institute of Zoology, Academia Sinca, Beijing, China.
Iwata, S., Saynovits, M., Link, T. A., and Michel, H. (1996). *Structure* **4**, 567–579.
Iwata, S., Lee, J. W., Okada, K., Lee, J. K., Iwata, M., Rasmussen, B., Link, T. A., Ramaswamy, S. and Jap, B. K. (1998). *Science* **281**, 64–71.
Junemann, S., Heathcote, P., and Rich, P. R. (1998). *J. Biol. Chem*, **273**, 21603–21607.

Kim, H., Xia, D., Yu, C. A., Kachurin, A., Zhang, L. Yu, L., and Deisenhofer, J. (1998). *Proc. Natl. Acad. Sci. U.S.* **95**, 8026–8033.
Link, T. A. and Iwata, S. (1996). *Biochim. Biophys. Acta* **1275**, 54–60
Mitchell, P. (1976). *J. Theoret. Biol.* **62**, 327–367.
Miki, T., Yu, L., and Yu, C. A. (1990). *Biochemistry* **30**, 230–238.
Ohnishi, T., Schagger, H., Meinhartdt, S. W., LoBrutto, R., Link, T. A., and von Jagow, G. (1989). *J. Biol. Chem.* **264**, 735–744.
Shenoy, S. K. Deng, K-P., Yu, L., and Yu, C. A. (1998). *Biophys. J.* **74**, 197a.
Tian, H., Yu, L., Mather, M W., and Yu, C. A. (1998). *J. Biol. Chem.* **273**, 27953–27959.
Tian, H., White, S., Yu, L., and Yu, C. A. (1999). *J. Biol. Chem.* **274**, 7146–7152.
Trumpower, B. L. (1990). *J. Biol. Chem.* **265**, 11409–11412.
Von Heijne, J., Steppuhn, J., and Herrmaan, R. G. (1989). *Eur. J. Biochem.* **180**, 535–545.
Ugulava, N. B., and Crofts, A. R. (1998). *FEBS lett.* **440**, 409–413.
Widger, W. R., Cramer, W. A., Herrmann, R. G., and Trebst, A. (1984). *Proc. Natl. Acad. Sci. U.S.* **81**, 674–678.
Xia, D., Yu, C. A., Kim, H., Xia, J.-Z, Kachurin, A. M., Zhang, L., Yu, L., and Deisenhofer, J. (1997). *Science* **277**, 60–66.
Yu, C. A., Xia, J-Z., Kachurin, A. M., Yu, L., Xia, D., Kim, H., and Deisenhofer, H. (1996). *Biochim. Biophys. Acta* **1275**, 47–53.
Yu, C. A., Xia, D., Kim, H., Deisenhofer, J., Zhang. L., Kachurin, A. M., and Yu, L. (1998). *Biochim. Biophys. Acta* **1365**, 151–158.
Yue, W. H., Yu, L., and Yu, C. A. (1991). *Biochemistry* **30**, 2303–230.
Zhang, L.,. Yu, L., and Yu, C. A. (1988). *J. Biol. Chem.* **273**, 33972–33976.
Zhang, Z. L., Huang, L.-S., Shulmeister, V. M., Chi, Y-I., Kim, K. K., Huang, L.-W., Crofts, A. R., Berry, E. A., and Kim, S. H. (1998). *Nature* **392**, 677–684.